

Experimental investigation on effect of partial flexibility at low aspect ratio airfoil - Part II: Installation both on suction and pressure surface

Kemal Koca^{1,*}, Mustafa Serdar Genç¹, Halil Hakan Açıkkel¹

¹Wind Engineering and Aerodynamic Research Center, Department of Energy Systems Engineering, Erciyes University, KAYSERİ, TURKEY

Abstract. In this experimental study, flow over NACA 4412 airfoil with flexible membrane mounted both on suction surface and pressure surface was investigated at Reynolds number of 5×10^4 and different angles of attack. The smoke-wire visualization method was used for flow visualization to demonstrate flow phenomena as laminar separation bubble (LSB), leading edge separation and tip vortices. A constant temperature anemometer (CTA) was used for measuring flow over the partially flexible airfoil. Concerning the flow visualization, smoke-wire experiment was been conducted at $z/c=0.1$ and $z/c=0.4$. Besides, hot-wire experiment by means of CTA was employed to measure flow properties including values of velocity, turbulence statistics and Reynold stress over both uncontrolled and controlled airfoil. The results showed that partially flexible airfoil had several benefits compared with the uncontrolled airfoil. The results for this partially flexible airfoil were mainly lower size of LSB, higher stall angle of attack, ensuring more stable flow characteristics and more aerodynamic performance.

1 Introduction

Air vehicles such as Unmanned Air Vehicles (UAVs) and wind turbines operate at lower Reynolds (Re) number [1-5]. At low Re number flows, the prediction, determination and controlling of LSB and transition phenomenon is important, because these low Re number flow phenomenon cause aerodynamic performance to decrease, blade/wing vibration to increase [6-24]. Therefore, nowadays researchers have focused experimental [18-21] and numerical [25-28] studies on the prediction, determination and controlling of LSB and transition phenomenon. Flexibility recently developed flow control technique [23-24], has been begun attention recently. Stall delaying and performance increasing as well as blade/wing stability can be provided with the utilizing of flexibility over air vehicles [23].

This experimental study is on a NACA 4412 wing with partial flexibility on both suction and pressure surfaces at $Re=5 \times 10^5$ and different angles of attack. The purpose of this study is to determine controlling of the flow using partially flexibility.

2 Experimental Setup

It was conducted at the wind tunnel with test section of 500mm by 500mm in Erciyes University. Free-stream turbulence intensity is under 0.7% [13]. The wing is with an 18 cm chord and 18 cm span length. The partial flexible wing was manufactured using a 3D printer. Figure 1 shows the wing with flexibility mounted between $x/c=0.2$ and $x/c=0.7$ because of the control of LSB and separation affects. The flexible membrane is latex rubber sheet [23] with the thickness of 0.2 mm. It was glued to the wing with double side tape.

The experimental study was carried out with the smoke wire flow visualization and flow measurements using a hot-wire system. Flow visualization was captured along $z/c=0.1$ (to see tip vortices) and $z/c=0.4$ (to see LSB formation) using a camera and illumination system. X wire probe was used in the hot-wire system at the over and wake of the wing. 20480 data were collected with a sample rate of 2 kHz at selected positions. Experimental details have been explained in Part-I of the study.

* Corresponding author: kemalkoca@erciyes.edu.tr

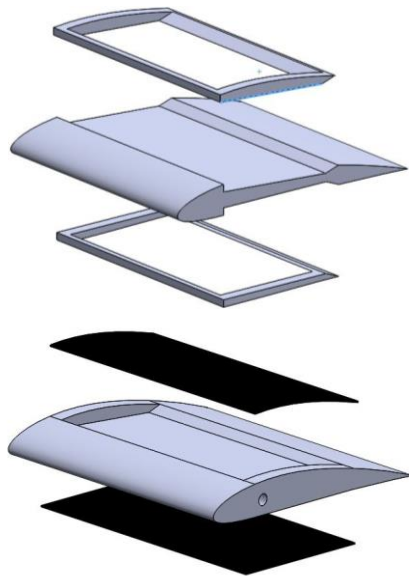


Fig. 1. The wing with flexibility on both suction and pressure surfaces.

3 Results

3.1 Velocity measurement results

Figure 2 and Figure 3 show dimensionless velocity distribution around the partial flexible wing at the about middle and tip of the wing. As seen from these figures, there is a short LSB over the wing, and the trailing edge separation formed at the rear of the wing. It was shown in Part-I that the flow separated at $x/c=0.2$ and reattached at $x/c=0.8$ in the uncontrolled case. The LSB was suppressed with the partially flexibility, and it is clearly seen that size of LSB was reduced. Flexible membrane vibration caused the flow to control with momentum transfer.

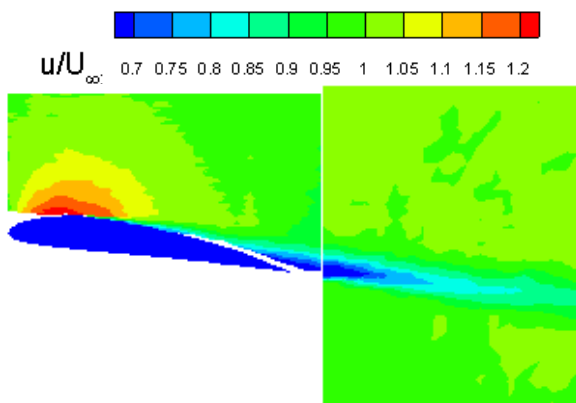


Fig. 2. u/U_∞ at $Re=5 \times 10^4$ and $\alpha=8^\circ$ for partial flexible wing (and $z/s=0.4$).

The long LSB formed due to adverse pressure gradient in uncontrolled case, controlled via flexible membranes on both suction and pressure surfaces. This causes the increase of lift and aerodynamic performance.

Distributions of turbulent intensity (Tu) and Reynolds stresses (Re stress) for partially flexible wing are given in Figure 4. Different contour colours at both Reynolds stress and turbulent intensity indicate changing in the flow-field. The transition to turbulence phenomenon formed at the middle of the wing during the streamwise location. In addition, the trailing edge separation was shown at the rear via the increasing in distribution of both Reynolds stress and turbulent intensity. Unlike the uncontrolled case, fluctuations because of vortex sheds at near wake are less, meaning less drag force and steadier flow in terms of aerodynamic performance.

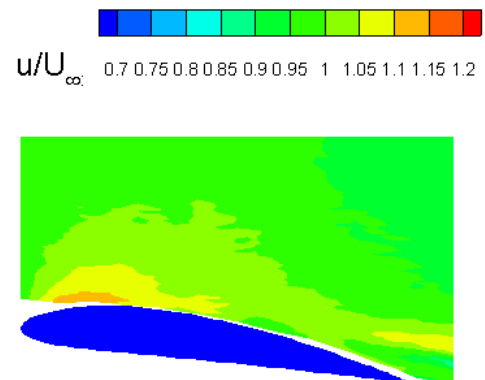


Fig. 3. u/U_∞ at $Re=5 \times 10^4$ and $\alpha=8^\circ$ for partial flexible wing (and $z/s=0.1$).

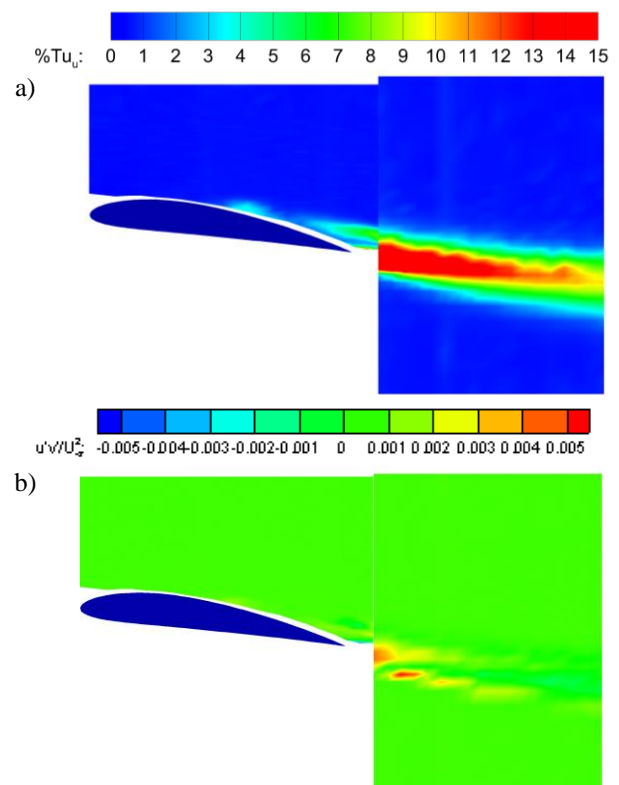


Fig. 4. a) Tu and b) Re stress at $Re=5 \times 10^4$ and $\alpha=8^\circ$ for partial flexible wing (and $z/s=0.4$).

3.2 Flow visualization results

In the smoke-wire flow visualization experiment, the flow pictures around the wing were taken by the camera.

In Figure 5, the photos for partial flexible wing at $\alpha=8^\circ$ in the middle of the wing ($z/s=0.4$) and the tip of the wing ($z/s=0.1$) were given. The long bubble seen in the uncontrolled case was suppressed with the partially flexibility, and the trailing edge separation formed at the rear of the wing. As the angle of attack increased, the flow over the wing started to separate and the tip vortex moved towards the leading edge of the wing as seen in Figure 6 ($\alpha=12^\circ$). Then, the flow separation enlarged at the higher angles of attack ($\alpha=20^\circ$) in Figure 7. Besides, the tip vortex grew up and the flow separation at the tip of the wing suppressed. Consequently, using the partial membrane over both two surfaces of the wing caused aerodynamic performance to increase.

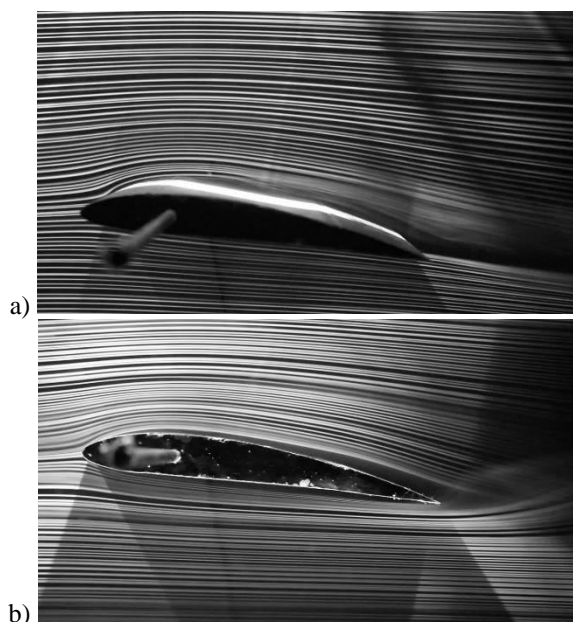


Fig. 5. At $\alpha=8^\circ$, smoke-wire photos for partial flexible wing at the plane of a) $z/s=0.4$ b) $z/s=0.1$.

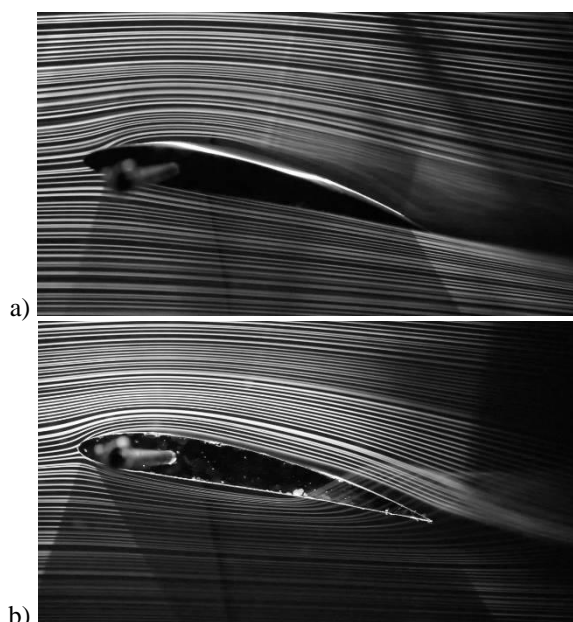


Fig. 6. At $\alpha=12^\circ$, smoke-wire photos for partial flexible wing at the plane of a) $z/s=0.4$ b) $z/s=0.1$.

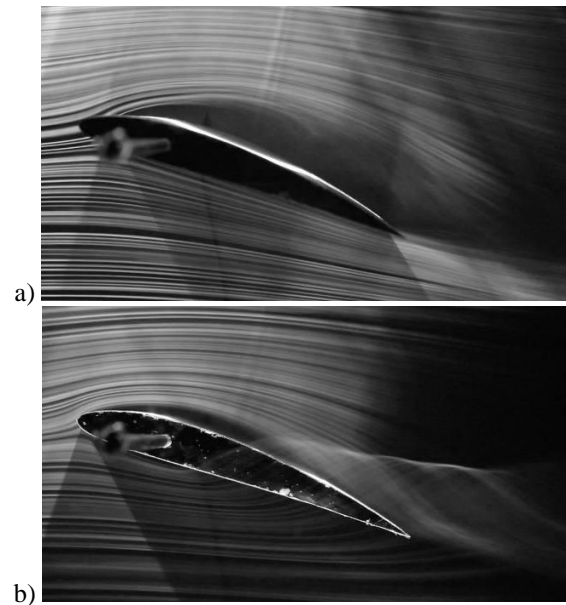


Fig. 7. At $\alpha=20^\circ$, smoke-wire photos for partial flexible wing at the plane of a) $z/s=0.4$ b) $z/s=0.1$.

4 Conclusion

In this study, the flow on AR=1 NACA4412 wing with the partial flexibility over both the suction and pressure surfaces were investigated at $Re= 5 \times 10^4$ and different angles of attack. The experiments were done using the smoke wire flow visualization technique and a hot-wire system for velocity measurement. Flow visualization was captured along $z/c=0.1$ for tip vortices effects and $z/c=0.4$ LSB formation and the leading-edge separation. In the hot-wire system, X wire probe was used at the over and wake of the wing. Although the laminar separation bubble and flow separation formed due to adverse pressure gradient were observed in the uncontrolled case at $\alpha=8^\circ$, $\alpha=12^\circ$, $\alpha=20^\circ$, the controlled cases showed that the flow was controlled and suppressed by using the partial flexible membrane material between $x/c=0.2$ and $x/c=0.7$ over both upper and lower surfaces of the wing. Unlike the partial flexibility over the suction surfaces of the wing, the flexibility on the pressure surfaces caused extra eddies to form at the lower region of the wing as seen in Figure 4b. These extra eddies provided to occur a vacuum effect at the wake of the wing, which supplied to control the flow.

References

1. Tani I, Prog Aerosp Sci, 5: 70–103, (1964).
2. Gaster, M. Aeronautical Research Council Reports and Memoranda, No: 3595, London, (1967).
3. T.J. Mueller, J.D. DeLaurier. Annual review of fluid mechanics, **35(1)**, 89-111 (2003)
4. Greenhalgh, S., Curtiss, H. C., Smith., AIAA journal, **22(7)**, 865-870 (1984).

5. M.S., Genç, I. Karasu, H.H. Açıkkel, M.T., Akpolat. In Low Reynolds number aerodynamics and transition. InTech. (2012)
6. Ke, S., Zhigang, W., Chao, Y., Chin. J. Aeronaut. **21(5)**, 402-410 (2008).
7. Zhang, Wei, Rainer Hain, and Christian J. Kähler. Experiments in fluids, **45, 4** 725-743 (2008).
8. Savaliya, Samir B., S. Praveen Kumar, and Sanjay Mittal. International Journal for Numerical Methods in Fluids **64(6)**, 627-652, (2010).
9. Hain R., Kahler C., Radespiel J., Journal of Fluid Mechanics, **630**, 129–153 (2009).
10. Mizoguchi, M., and Itoh H. AIAA journal **51(7)**, 1631-1639 (2013).
11. Shields, M. and Mohseni K. AIAA journal **50(1)** 85-99 (2012).
12. Y. Lian, W. Shvy, D. Viieru, B. Zhang. Progress in Aerospace Sciences, **39(6-7)**, 425-465 (2003)
13. M.S. Genç, I. Karasu, H.H. Açıkkel, Experimental Thermal and Fluid Science, **39**, 252-264, (2012).
14. K. Koca, M.S. Genç, H.H. Açıkkel, M. Çağdaş, T.M. Bodur. Energy, **144**, 750-764 (2018)
15. L. E. Jones, R. D. Sandberg, N. D. Sandham. J. Fluid Mech., **602**, 175-207, (2008).
16. M. S. Genç, K. Koca, H. H. Açıkkel, G. Özkan, M. S. Kırış, R. Yıldız. In EPJ Web Conf., **114**, 2029, (2016).
17. A. Ducoin, J. C. Loiseau, J. C. Robinet. Eur. J. Mech: B/Fluids, **57**, 231-248, (2016).
18. H.H. Açıkkel, M.S. Genç. Proc IMechE, Part G: Journal of Aerospace Engineering, **230(13)**, 2447-2462 (2016).
19. M.S. Genç. H.H. Açıkkel, M.T. Akpolat, G. Özkan, İ. Karasu, Journal of Aerospace Engineering-ASCE, 29 (6), 04016045, 2016.
20. H. Wang, B. Zhang, Q. Qiu, X. Xu. Energy, **118**, 1210-1221 (2017)
21. M.S. Genç, K. Koca, H.H. Açıkkel. Energy, **176**, 320-334 (2019)
22. M.S. Genç, G. Özkan, M. Özden, M.S. Kırış, R. Yıldız. Proc IMechE, Part C: Journal of Mechanical Engineering Science, **232(22)**, 4019-4037 (2018)
23. H.H. Açıkkel, M.S. Genç. Energy, **165**, 176-190 (2018)
24. H. Demir, M.S. Genç, European Journal of Mechanics B/Fluids, **65**, 326-338 (2017).
25. M.S. Genç, U. Kaynak, H. Yapıcı, European Journal of Mechanics B/Fluids, **30(2)** 218-235 (2011).
26. M.S. Genç, Proc IMechE, Part C- Journal of Mechanical Engineering Science, **Vol 224 (10)**, pp. 2155 – 2164, 2010.
27. I. Karasu, M. Özden, M.S. Genç, Journal of Fluids Engineering-Transactions of The ASME, **140(12)** 121102-1-121102-15 (2018).
28. K. Koca, M.S. Genç, H.H. Açıkkel. Çukurova Üniversitesi Mühendislik-Mimarlık Fakültesi Dergisi, **31(ÖS2)**, 127-134 (2016)